ARTICLE

Optimized Allotopic Expression of the Human Mitochondrial *ND4* Prevents Blindness in a Rat Model of Mitochondrial Dysfunction

Sami Ellouze,[1] Sébastien Augustin,[1] Aicha Bouaita,[1] Crystel Bonnet,[1] Manuel Simonutti,[1] Valérie Forster,[1] Serge Picaud,[1] Jose-Alain Sahel,[1] and Marisol Corral-Debrinski[1,*]

Mitochondrial diseases due to mutations in mitochondrial DNA can no longer be ignored in most medical areas. With prevalence certainly higher than one in 6000, they probably represent the most common form of metabolic disorders. Despite progress in identification of their molecular mechanisms, little has been done with regard to therapy. We have recently optimized the allotopic expression for the mitochondrial genes *ATP6*, *ND1*, and *ND4* and obtained a complete and long-lasting rescue of mitochondrial dysfunction in the human fibroblasts in which these genes were mutated. However, biosafety and benefit to mitochondrial function must be validated in animal models prior to clinical applications. To create an animal model of Leber Hereditary Optic Neuropathy (LHON), we introduced the human *ND4* gene harboring the G11778A mutation, responsible of 60% of LHON cases, to rat eyes by in vivo electroporation. The treatment induced the degeneration of retinal ganglion cells (RGCs), which were 40% less abundant in treated eyes than in control eyes. This deleterious effect was also confirmed in primary cell culture, in which both RGC survival and neurite outgrowth were compromised. Importantly, RGC loss was clearly associated with a decline in visual performance. A subsequent electroporation with wild-type *ND4* prevented both RGC loss and the impairment of visual function. Hence, these data provide the proof-of-principle that optimized allotopic expression can be an effective treatment for LHON, and they open the way to clinical studies on other devastating mitochondrial disorders.

Introduction

Mitochondrial diseases encompass an extraordinary assemblage of clinical problems, commonly involving tissues that have high energy requirements, such as retina, brain, heart, muscle, liver, and endocrine systems. The clinical presentations range from fatal infantile disease to muscle weakness, and most are characterized by inexorable progression.[1] Moreover, mitochondrial dysfunctions also contribute directly or indirectly to tumor formation and the aging process.[1,2] Approximately 300 mtDNA alterations have been identified as the genetic cause of mitochondrial diseases; one-third of these alterations are located in coding genes for oxidative phosphorylation (OXPHOS) proteins.[3] Recent epidemiological studies have shown that mtDNA-related disease prevalence is at least one in 6000.[4] The understanding of the pathogenesis of mitochondrial diseases has improved considerably in the last decade. Nevertheless, the most disappointing area is the lack of efficient treatments for patients with mitochondrial diseases. Indeed, they are still treated with vitamin and cofactor mixtures, which are harmless but largely inadequate and inefficient.[5]

Leber hereditary optic neuropathy (LHON [MIM 535000]) was the first maternally inherited disease associated with point mutations in mitochondrial DNA (mtDNA)[6] and is now considered the most common mitochondrial disorder, with an estimated prevalence of 1 in 25,000 in north-east England.[7,8] It has recently been reported that LHON might be responsible for as much as 2% of blindness in individuals under age 65.[9] The pathology is characterized by selective death of retinal ganglion cells (RGC) and optic nerve atrophy, leading to central vision loss. The most common pathogenic mutations found in about 95% of LHON patients are located in *ND1* (G3460A) [MIM 516000], *ND4* (G11778A) [MIM 516003], or *ND6* (T14484C) [MIM 516006] genes. They encoded subunits of the respiratory chain complex I, and the mutations have the double effect of lowering ATP synthesis and increasing oxidative stress chronically.[10]

For diseases caused by mutations in mtDNA, such as LHON, allotopic expression (expression of mitochondrial genes transferred to the nucleus) of some of them has been tried in vitro as a potential therapeutic option.[11,12] However, several attempts failed to obtain complete and long-lasting rescue of mitochondrial defects in cultured cells carrying mutations of mtDNA genes.[13,14] We have recently optimized the allotopic expression for the mitochondrial genes *ATP6* [MIM 516060], *ND1*, and *ND4* and obtained a complete and long-term restoration of mitochondrial function in human fibroblasts in which these genes were mutated. This optimization was reached by mRNA targeting to the mitochondrial surface, which lead to a tight coupling between both translation and translocation processes; this tight coupling is required for highly hydrophobic proteins, such as ATP6, ND1, and ND4.[15,16]

The next mandatory step before any attempt to clinical application of our strategy is to provide the proof-of-principle that our vectors are both safe and beneficial to mitochondrial function in vivo. Unfortunately, the major

obstacle to this goal is the lack of a reliable animal model faithfully recapitulating the main characteristics of human diseases due to mtDNA mutations.[5] Our aim was to create an experimental model of LHON; therefore, we used the optimized-allotopic-expression approach and in vivo electroporation (ELP)[17] to introduce on adult rat eyes the human *ND4* gene harboring the G11778A substitution. This mutation, responsible for 60% of LHON cases, converts a highly conserved arginine to histidine at codon 340.[10] Histological evaluation of these animal retinas showed a significant decrease (30%–40%) in the overall number of RGCs compared to those in animals in which in vivo ELP was performed with either wild-type *ND4* or the green fluorescence protein (GFP). The decreased number of RGCs was associated with impaired visual function. Remarkably, RGC loss was rescued by a second ELP with the wild-type *ND4* gene and prevented a decline in visual function. These data represent the "proof of principle" that optimized allotopic expression is effective in vivo and can be envisaged as a therapy for mtDNA-related diseases.

Material and Methods

Animals

Male Wistar and Long Evans rats (Janvier, Le Genest Saint Isle, France) of 8–14 weeks of age (250–300 g) were housed two per cage in a 12 hr light/12 hr dark cycle and were fed water and dried rations ad libitum. Experiment protocols were developed in accordance with the ARVO (Association for Research in Vision and Ophthalmology) Statement for the Use of Animals in Ophthalmic and Visual Research.

Plasmid Construction

The optimized human wild-type *ND4* ORF fused to the first 84 nucleotides of the human *COX10* [MIM 602125] ORF was obtained as previously described.[15,16] The *COX10* fragment encodes the 21 residue N-terminal mitochondrial targeting sequence (MTS) and seven additional residues that ensure proper MTS cleavage (MAASPHTLSSRLLTGCVGGSVWYLERRT). Using the Quick Change Multi Site-Directed Mutagenesis Kit (Stratagene, USA) and the primer CTACGAAAGGACACACTCACACATTATGATTCT GAGCCAGG, we performed in vitro mutagenesis of the wild-type engineered human *ND4* gene to obtain a nuclear version harboring the G11778A substitution.

We cloned the fusion *COX10-ND4* sequences into the pAAV-IRES-hrGFP vector (Stratagene) by using BamHI and XhoI. In the recombinant vectors three FLAG epitopes are appended in frame to the C terminus of ND4 proteins. To obtain hybrid mRNAs that also contained the *COX10* 3′ UTR, we replaced the hGH (human growth hormone 1 [MIM 139250]) poly adenylation signal of the vector with the 1425 bp full-length *COX10* 3′ UTR by using BglII and RsrII sites. Final constructs were sequenced for accuracy (Genome Express, France). DNA purifications for in vivo ELP were performed with the QIAprep Maxiprep Kit Endofree (QIAGEN) according to the manufacturer's instructions. DNAs were diluted in TE buffer (10 mM Tris [pH 7.5]; 1 mM EDTA) at a final concentration of 5 mg/ml.

The hrGFP gene serves as a useful marker for detecting cells expressing the transgene. The corresponding protein is a humanized *Renilla reniformis* protein that is less toxic than the jellyfish *Aequorea victoria* EGFP protein. However, because the gene is located downstream from the IRES, its expression is low, as reported by the manufacturer. Hence, hrGFP fluorescence was evaluated with an antibody against GFP.

In Vivo Electroporation

The electroporation procedure was performed essentially as described by Ishikawa and colleagues[17] but with some modifications. Under anesthesia with isoflurane (40 mg/kg body weight), 20 μg of DNA (4 μl and 1/10 of fluorescein) were injected into the vitreous body with a 30 gauge needle 0.5 mm posterior to the limbus after dilation of the pupil. After 5 min the contact-lens-type and needle electrodes were positioned, and square wave pulses were delivered. Electric pulses were generated by an Electro Square Porator (T830; BTX, San Diego, CA USA). Conditions were as follows: electric field strength of 9 V/cm, pulse duration of 100 ms, and a stimulation pattern of five series of electric pulses with frequency of one pulse per second, interrupted by 5 min pauses in-between. ELPs were performed in only one eye per rat. Eye fundus images were captured the day after the procedure and before animal sacrifices to ensure the technique safety. One percent of examined animals developed cataracts and were excluded from further analyses. RGCs were purified from 228 animals for ex vivo studies and RT-PCR analyses. RGC counts were performed in 150 electroporated animals. Retinal sections from 12 electroporated animals were subjected to a TUNEL assay. Retinal whole mounts from 12 animals that had been subjected to in vivo ELP were processed for immunohistochemistry with NF200. Visual performances of 46 animals subjected to ELP were monitored with an optomotor test. Within this animal group after the animals' sacrifice, 32 were used for RGC counting, 8 retinal whole mounts were performed, and 6 retinas were subjected to TUNEL assay.

Histology and RGC Counts

Animals were sacrificed by transcardiac perfusion with 4% paraformaldehyde (PAF) under deep ketamine (50 mg/kg) and xylazine (10 mg/kg) anesthesia. The globes were removed from the animal, a small marking burn apart from the retina was placed on the eyes for the identification of retinal orientation, and the eyes were then pierced in the cornea with a needle and fixed for 1 hr in 3% PAF at 4°C. After the first fixation, the cornea and lens were removed and postfixed overnight in 4% PAF at 4°C. Next, eyes were cryoprotected for 1 hr in 20% sucrose-PBS (Sigma-Aldrich) at 4°C and overnight in 30% sucrose-PBS at 4°C. The next day, retinas were embedded in OCT (Neg 50; Richard-Allan Scientific), frozen in liquid nitrogen, and stored at −20°C. Sections (10 μm thick) were cut on a Microm Cryostat (Microm Microtech, France) at −20°C and mounted on SuperFrost@Plus slides (Menzel-Gläser, Germany). Nine slides were obtained per eye; each slide contained six consecutive sections from the superior side. Because DNA injection was performed on the superior side and the RGC population increases near the optic nerve (ON) [18], RGC counts were performed from each retina on four entire consecutive cryostat sections with the same deepness at 400 μm from the ON. Cryostat sections of retinas were washed with PBS, permeabilized with 0.1% Triton X-100 in PBS for 5 min at room temperature, and treated with 0.1% bovine serum albumin (BSA [Sigma-Aldrich]) and 0.1% Tween 20 in PBS for 1 hr so that nonspecific binding sites would be blocked. The

retinas were then incubated with polyclonal rabbit antibody against NF200 (1 µg/ml, Sigma-Aldrich) or against GFP (1.5 µg/ml, Torrey Pines Biolabs, USA) and either monoclonal mouse antibody against BRN3a (1 µg/ml, Chemicon) or monoclonal FLAG (2.5 µg/ml, F3165, Sigma-Aldrich) overnight at 4°C. Next, sections were washed three times in PBS and incubated with DAPI (2 µg/ml; Sigma-Aldrich) and appropriate secondary antibodies conjugated with monoclonal mouse 594 (4 µg/ml, Invitrogen) or goat anti-rabbit 488 (4 µg/ml, Invitrogen) for 1.5 hr at room temperature. We performed negative control experiments by incubating retinal sections with each secondary antibody. Three or four persons who were masked with regard to the identity of experimental and control eyes estimated RGC numbers with the help of Image J software.

TUNEL Assay

Four consecutive cryostat sections corresponding to 400 µm from the ON were chosen, and a TUNEL assay was performed with the in situ apoptosis detection kit (Roche, Penzberg, Germany) according to the manufacturer's instructions. For the positive control, the sections were treated with DNase. The number of TUNEL-positive cells per section was obtained from the counting of colocalization between DAPI and TUNEL stainings. Six animals were used for each condition.

Retinal Whole Mounts and Immunochemistry

Rat eyes were enucleated; the anterior segment, the lens, and the vitreous body were rapidly removed; and eyes were fixed overnight with 4% PAF. After three washes in PBS, retinas were incubated in 3% BSA (Sigma-Aldrich) and 0.05% Tween-20 (Sigma-Aldrich) for 20 min. Next, retinas were permeabilized with 0.1% Triton X-100 for 5 min, rinsed with PBS, and incubated with polyclonal NF200 antibody (1 µg/ml, Sigma-Aldrich) overnight at 4°C. After three washes with PBS, they were treated with the secondary antibody goat anti-rabbit 488 (4 µg/ml, Invitrogen) and DAPI (2 µg/ml, Sigma-Aldrich) for 1.5 hr and finally washed three times in PBS. The eye cup was cut peripherally in four sections under a binocular optic microscope and flattened. The sclera/choroid/RPE was removed with fine forceps, and the neuroretina was mounted on a glass slide and examined by fluorescence microscopy. Twelve electroporated eyes were observed and compared to four control eyes.

Purification of RGCs for Primary Cultures and Semiquantitative RT-PCR Analyses

Primary cell cultures were derived from adult rat retinas and purified by modifications of the sequential immunopanning described for young rats.[19] RGCs and macrophages were resuspended in half NBA medium (Invitrogen) supplemented with B27 (1:50; Invitrogen) and L-glutamine (2 mM; Invitrogen) and half rat-retinal cell-conditioned culture medium,[20] and seeding was performed at 20,000 cells/cm^2 into 48-well tissue-culture plates containing coverslips previously coated overnight with poly-D-lysine (2 µg/cm^2 for 1 hr) and then with laminin (1 µg/cm^2 overnight: both from Sigma-Aldrich). Cells were incubated at 37°C in a humidified atmosphere of 5% CO$_2$. Ten days later, cells were fixed with 4% PAF solution for 15 min at room temperature and washed three times in PBS before immunocytochemistry analyses were performed. Coverslips containing RGCs were permeabilized with 0.1% Triton X-100 in PBS for 5 min at room temperature and treated with 0.1% BSA (Sigma-Aldrich) and 0.1% Tween-20 (Sigma-Aldrich) in PBS for 1 hr so that nonspecific binding sites would be blocked. Then, they were incubated with polyclonal rabbit antibody against NF200 (1 µg/ml, Sigma-Aldrich), monoclonal anti-ATP synthase subunit α (0.5 µg/ml, Invitrogen), or monoclonal anti-FLAG M2 (2.5 µg/ml, Sigma-Aldrich) overnight at 4°C. The next day, samples were washed and treated for 1.5 hr at room temperature with DAPI (2 µg/ml, Sigma-Aldrich) and appropriate secondary antibodies: labeled goat anti-mouse IgG1 Alexa Fluor 488 for the anti-Flag M2 antibody (2 µg/ml; Invitrogen), labeled goat anti-rabbit IgG1 Alexa Fluor 488 (2 µg/ml; Invitrogen) for the anti-NF200 antibody, and labeled goat anti-mouse IgG 2b Alexa Fluor 594 (2 µg/ml, Invitrogen) for the anti-ATP synthase subunit α antibody (Molecular Probes, Invitrogen). Cell counts have been performed manually and as blind tests with regard to animal identities after fluorescence microscopy observations. Estimations of cell body diameters and neurite lengths in cultured RGCs were performed with the Image J software.

For RT-PCR analyses, we extracted total RNAs with the RNeasy Protect Mini kit (QIAGEN) from 8×10^5 cells that we obtained by pooling 18 retinas subjected to RGC purification. RT-PCR analyses were performed with the Superscript III one-step RT-PCR Platinum Taq kit (Invitrogen). We estimated steady-state levels of different mRNAs by using 60 ng of total RNA from RGCs purified 25 days after ELP with GFP, wild-type *ND4*, or mutant *ND4* and specific primers (Table S1, in the Supplemental Data available with this article online). Twenty-five, 30, and 35 cycles of PCR amplification were performed with three independent RNA purifications. The intensity of PCR products was quantified with the Quantity One 1-D Analysis Software (Bio-Rad Laboratories, USA).

Microscopic Observations

Fluorescence labeling was monitored with a fluorescence microscope (Leica DM 5000 B). Magnifications of 200×, 400×, or 630× were used for the acquisition of images with the MetaVue software. The images were analyzed with Photoshop and Image J software.

Optomotor Tests

The head-tracking method is based on an optomotor test devised by Cowey and Franzini in 1979[21] and frequently used since then.[22,23] Eight-, 12-, or 14-week-old Long Evans rats were placed individually into an enclosed clear plastic container, surrounded by a motorized drum that could revolve clockwise or counterclockwise. Each animal was placed in a clear plastic stationary round chamber at the center of the drum, which allows visualization and exposure of both eyes to the stimulus. A single blinded operator conducted all assessments, and codes were broken upon completion of data acquisition. The operator waited for the animal to settle in the chamber before initiating drum rotation. Vertical black-and-white lines of three varying widths, subtending 0.125, 0.25, and 0.5 cycles/degree (cyc/deg) were presented to the animal and rotated alternatively clockwise and counterclockwise, each for 60 s. This stimulated a subcortical reflex, so that a seeing animal involuntarily turned its head to track the moving lines. Head movements were recorded with a video camera mounted above the apparatus. Animals were scored only when the speed of the head turn corresponded to the speed of rotation of the stripes (12°/s). Habitual and other seemingly randomized movement was excluded from the timing. Light levels were kept constant (240 lux), and the plastic container was cleaned between animals. Each animal was tested at two different time points by a single observer. During the experiments, a second masked grader
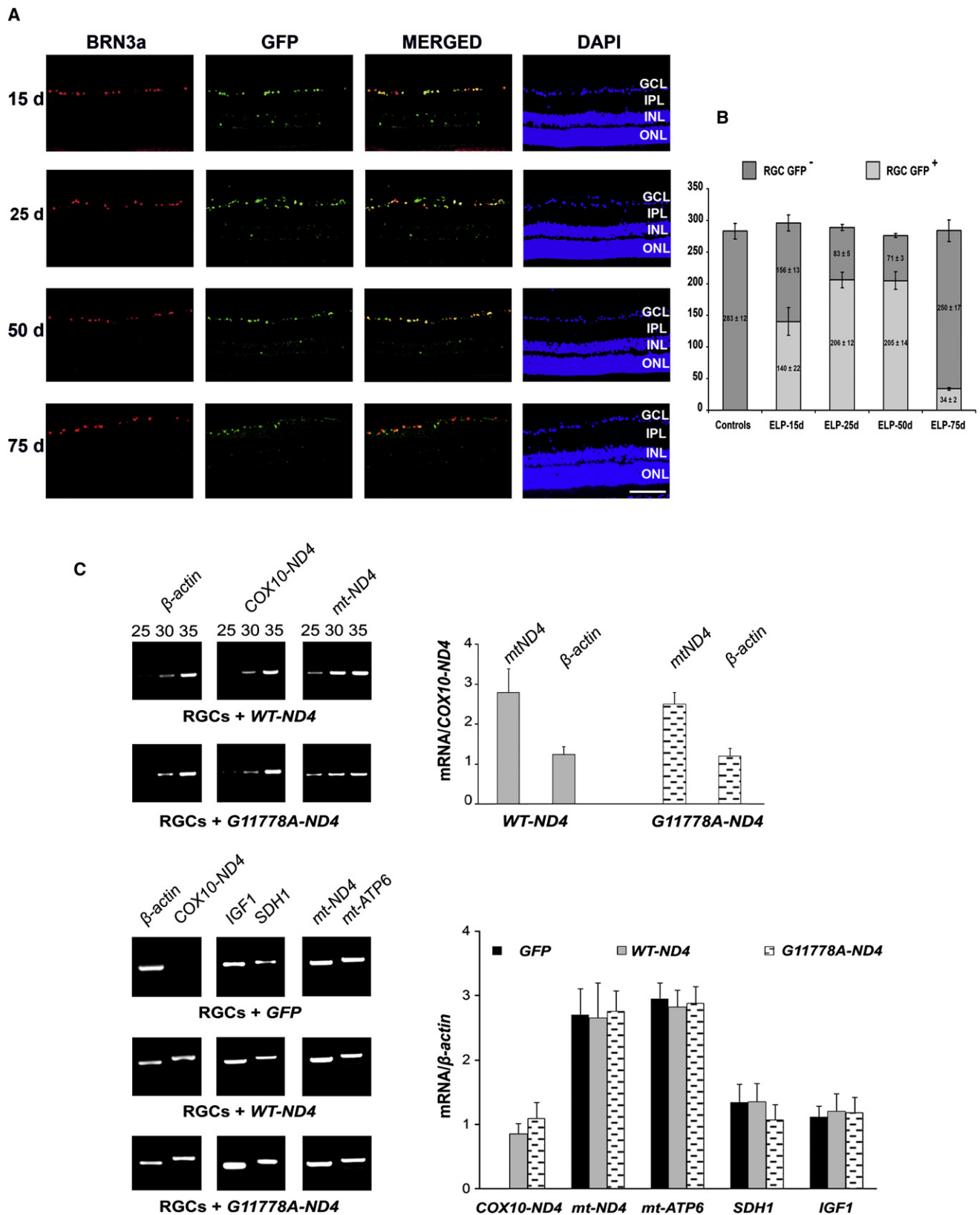
Figure 1. Efficacy of Gene Transduction for In Vivo ELP

(A) Immunofluorescence analyses with antibodies to BRN3a and GFP of cryostat retinal sections from animals electroporated with the GFP vector. Six animals were sacrificed 15, 25, 50, and 75 days after the intervention. GCL, ganglion cell layer; IPL, inner plexiform layer; INL, inner nuclear layer; ONL, outer nuclear layer. Scale bars represent 50 μm.

re-evaluated the video recording to confirm the reliability of the scoring system. Scores obtained from half of the control rats shown in Figure 5A represented a subgroup of the animals just before in vivo ELP; these animals were subjected to the optomotor test before sacrifice, and their scores are shown in Figures 5C and 5D.

Statistical Analyses

Values are expressed as means ± standard error of the mean (SEM). Data were compared via the Student's t test for all kinds of counts. p values of <0.05 were regarded as significant, and those <0.01 were regarded as highly significant.

Results

Gene Transfer into RGCs by In Vivo Electroporation

Gene introduction efficacy by in vivo ELP[17] was evaluated in RGCs over time. Six animals electroporated with the gene encoding the green fluorescent protein (hrGFP) under the control of the human cytomegalovirus promoter were sacrificed 15, 25, 50, and 75 days after in vivo ELP. To evaluate the number of RGCs expressing the GFP, we immunostained cryostat sections of retinas with GFP and BRN3a antibodies. *BRN3a* encodes a neuron transcription factor exclusively expressed in RGCs.[24] RGC-positives for both antibodies were counted in four independent retinal sections per animal. GFP immunostaining was mainly appreciated in the ganglion cell layer (GCL), indicating that DNA injection in the vitreous body and subsequent in vivo ELP effectively delivered DNA to the GCL. Some GFP-positive cells, possibly amacrine cells, were also seen in the inner nuclear layer (INL) (Figure 1A). The proportion of GFP-positive cells among the total BRN3a-labeled population in the GCL increased over time up to day 50 (Figure 1B). At 25 and 50 days, more than 70% of the cell population that immunostained with the Brn3A antibody were also immunoreactive to the GFP antibody. When animals were sacrificed 75 days after in vivo ELP, the longest period examined, GFP expression was strongly reduced; indeed, only 12% of BRN3a-immunostained RGC somas remained GFP positive, indicating the nucleus-degradation of DNA molecules from the vector at that time point. Light-microscopic observations of retinal sections revealed neither structural impairments nor inflammatory responses at different times after in vivo ELP (data not shown). Additionally, the overall number of RGCs in eletroporated eyes was not statistically different from that in controls; according to Student's t test p values were 0.66, 0.83, 0.67, and 0.97 for animals sacrificed 15, 25, 50, and 75 days after ELP (Figure 1B). Because in vivo ELP was an effective and sustainable method for introducing DNA into RGCs without noticeable cell damage, we used it to create an animal model of LHON disease by introducing vectors leading to the optimized allotopic expression of the human mitochondrial *ND4* gene, as recently reported.[15,16] By in vitro mutagenesis of the wild-type engineered human *ND4* gene, we obtained a nuclear version harboring the G11778A substitution. Both wild-type *ND4* and its mutant counterpart were combined with the two mRNA targeting sequences of human *COX10*, which ensures the efficient sorting of the mRNAs to the mitochondrial surface.[15,16] To estimate the efficiency of our constructions on directing the expression of nuclearly encoded *ND4* genes, we performed in vivo ELP in one eye of 18 animals with GFP, mutant, or wild-type *ND4*. Animals were sacrificed 25 days later, and total RNAs were obtained from purified RGCs. Steady-state levels of hybrid mRNAs (*COX10-ND4*) were compared to endogenous *ND4* and β-actin mRNAs by semiquantitative RT-PCRs after 25, 30, and 35 cycles of amplification. The quantification of signals obtained indicated that levels of transgene *ND4* and β-actin transcripts were similar, and almost 3-fold lower than endogenous *ND4* mRNA in RGCs expressing either wild-type or mutant *ND4* (Figure 1C, upper panel). Moreover, steady-state levels of hybrid mRNAs were comparable in cells allotopically expressing either of the *ND4* genes. We further examined the relative amounts of *COX10-ND4* mRNAs and two nuclearly transcribed mRNAs *IGF1* (encoding the insulin-like growth factor) and SD*H1* (encoding a mitochondrial protein of respiratory chain complex II), as well as the mitochondrially transcribed *ATP6* gene (which encodes a subunit of respiratory chain complex V). As expected, RGCs electroporated with GFP vector did not show any signal when primers for hybrid *ND4* mRNA were used. The relative levels of both *ATP6* and *ND4* genes transcribed from mtDNA were comparable in

(B) Numerical evaluation of data presented in (A). Four independent sections per animal were counted for BRN3a-positive cells in controls (RGC-GFP⁻); in electroporated animals the number of cells labeled with both BRN3a and GFP antibodies was estimated (RGC-GFP⁺). Mean ± SEM for six control rats and animals euthanized 15, 25, 50, or 75 days after in vivo ELP are shown.

(C) The steady-state levels of endogenous and hybrid *ND4* mRNAs were determined in purified RGCs from animals subjected to in vivo ELP with either mutant *ND4* (RGCs + G11778A-*ND4*), wild-type *ND4* (RGCs + WT-*ND4*), or the empty vector (RGCs + GFP) by RT-PCR. Upper panel: Semiquantitative estimations were made after 25, 30, and 35 cycles of PCR amplification with 60 μg of RNA as a starting material. Densitometric analyses were performed with signals revealed by electrophoresis (1/10 of the RT-PCR reaction) for three independent RNA extractions and two RT-PCRs per RNA. Bar graphs represented ratios ± SEM of either endogenous mtDNA *ND4* (*mtND4*) or β-actin signals to *COX10-ND4* signal obtained with RNA purified from RGCs expressing either mutant (G11778A-*ND4*) or wild-type *ND4* (WT-*ND4*). Bottom panel: Relative amounts of β-actin, *COX10-ND4, IGF1, SDH1, mtND4* and *mtATP6* mRNAs were evaluated after 30 cycles of PCR amplification of the reverse-transcribed products from 60 μg of RNAs obtained from RGCs expressing either mutant *ND4* (RGCs + G11778A-*ND4*), wild-type *ND4* (RGCs + WT-*ND4*), or the empty vector (RGCs + GFP). Bar graphs represent ratios ± SEM of *COX10-ND4, IGF1, SDH1, mtND4*, and *mtATP6* signals to β-actin signal. RT-PCR experiments were performed twice for three independent RNA extractions.

Specific oligonucleotides used for each gene are summarized in Table S1.
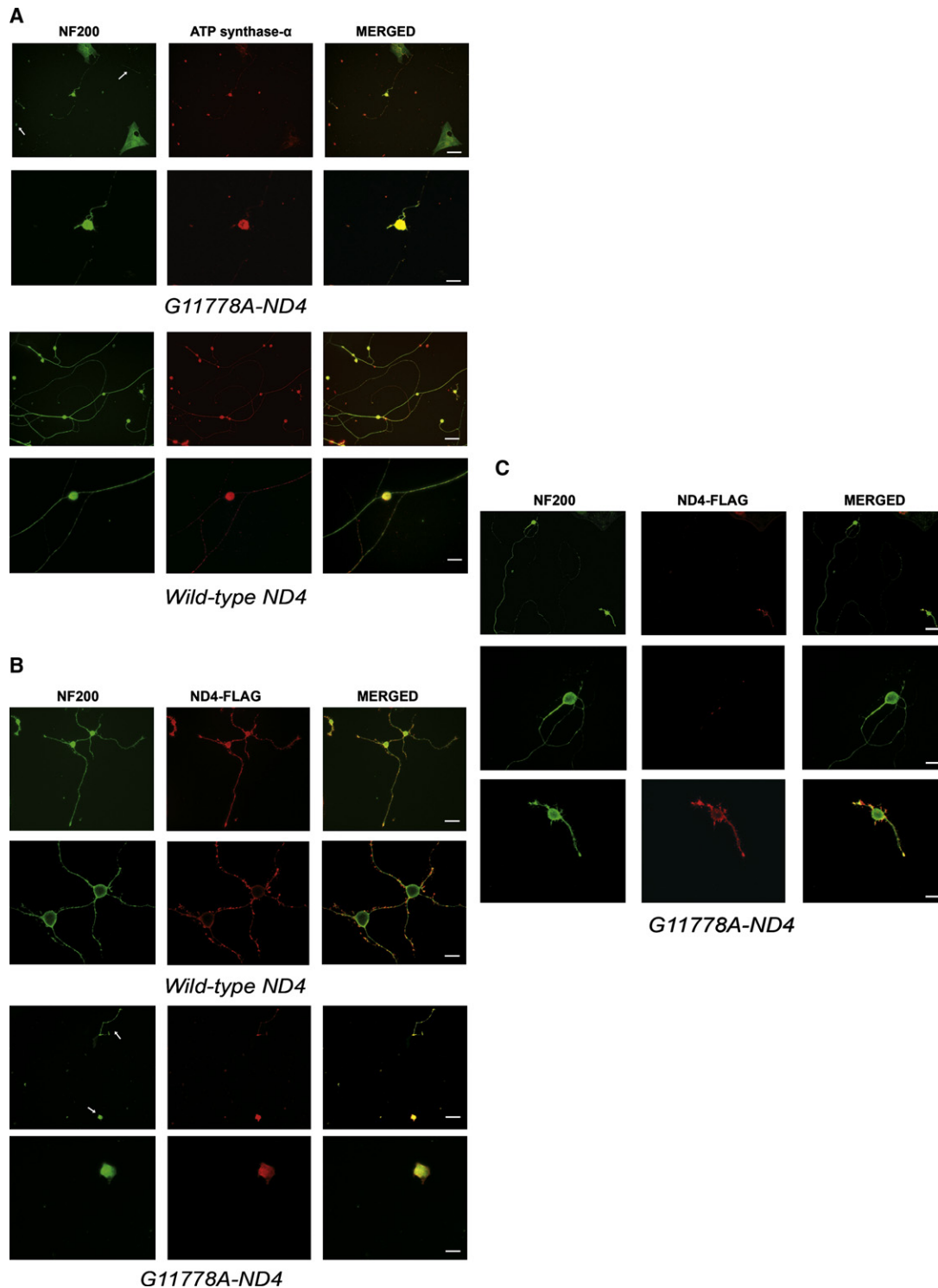
Figure 2. Ex Vivo Properties of RGCs Isolated from Electroporated Eyes

(A) RGCs were purified as previously described.[20] After 10 days of culture, cells were visualized by indirect immunofluorescence with antibodies against NF200 or ATP synthase α-subunit. RGCs were labeled essentially within their neurites; a clear difference in their lengths was noticed between cells purified from eyes expressing mutant *ND4* (G11778A-*ND4*) and those expressing wild-type *ND4*. The merged image of immunofluorescence revealed a significant colocalization of both NF200 and ATP synthase-α signals in cells examined. The scale bar represents 25 μm (magnification of 200×). A high-power view (magnification of 630×) featuring one of the cells immunolabeled with the antibodies is also presented for each condition; scale bars represent 8 μm.

(B) The subcellular localization of the allotopically expressed ND4 proteins was examined by indirect immunofluorescence with an antibody against the FLAG epitope (ND4-FLAG) in RGCs cultured for 10 days, and this was compared to signal obtained with the antibody against NF200. The merged image of immunofluorescence shows a significant colocalization of the fusion ND4 and NF200 proteins in

all cells evaluated and approximately 3-fold higher than either one of the nuclearly transcribed mRNAs tested (Figure 1C, bottom panel). Even though we are aware that *COX10-ND4* mRNA abundance would be underestimated given that not all of the RGCs analyzed expressed the transgenes (Figures 1A and 1B), these experiments allowed us to conclude that both engineered human *ND4* genes introduced into RGCs by in vivo ELP were efficiently transcribed. Therefore, we will be able to measure the impact on RGC function of the corresponding polypeptides.

Ex Vivo Properties of RGCs Isolated from Electroporated Eyes

In the few LHON cases that have been studied histopathologically, a drastic loss of RGC and nerve fiber layer (NFL) was the major retinal finding.[25] Therefore, we examined whether the in vivo expression of mutant *ND4* influenced RGC survival and neurite outgrowth in primary RGC cultures. For RGC purification, immunopanning was performed on eyes that expressed, for 25 days, either wild-type *ND4* or its counterpart bearing the G11778A substitution. The number of viable cells and their ability to develop neuritic processes were evaluated in six independent experiments, after 10 days of culture in rat retinal cell-conditioned medium.[20] We assessed cell survival by counting RGCs immunolabeled by the NF200 antibody, which recognizes the heavy subunit of intermediate neurofilaments; this subunit is specifically found in RGCs of several mammalian species.[26,27] In vivo expression of mutant *ND4* led to a consistent and significant decrease in the number of NF200-positive cells in culture as compared to in vivo expression of wild-type *ND4* (86 ± 9.6 and 237 ± 13.3 respectively, an approximate 3-fold decrease). The difference was significant according to a Student's t test (p value = 0.00016; n = 6). Notably, the majority of RGCs in cultures from eyes expressing wild-type *ND4* possessed multiple (three to six) processes that extended for many cell-body diameters and were often branched. Neurite lengths occasionally measured up to 500 µm. Interestingly, the neuritic processes from proximal cells tended to fuse as illustrated in Figure 2A (wild-type *ND4*). Immunoreactivity obtained with the antibody against the mitochondrial ATP synthase α-subunit was similar to the one observed with the NF200, indicating that mitochondria were distributed along the neuritic processes and in the cytosol (Figure 2A). Cultured RGCs from eyes electroporated with mutant *ND4* were scarce

and generally had no more than two short neurites. NF200-positive somas devoid of processes and neurites not associated with cell bodies were often seen, suggesting that by the end of the experiment cells had died (Figures 2A and 2B, G11778A-*ND4* arrows). Counting the number of NF-200-positive cells presenting at least one process that extended for around four soma diameters showed a clear difference between RGCs under the two conditions examined (17 ± 7.5 and 201 ± 10.3 for mutant *ND4* and its wild-type counterpart, respectively). Fewer than 20% of RGCs purified from eyes electroporated with mutant *ND4* developed long neurites, whereas approximately 85% of RGCs from eyes electroporated with wild-type *ND4* did so. RGC expression of *ND4* genes 35 days after the electroinduction was evaluated with FLAG antibody (Figure 2B). Most of the cells purified from eyes electroporated with either version of the *ND4* gene were labeled with the antibody. This immunoreactivity was consistently found in both cell bodies and neurites independently of their length. There was a clear colocalization of NF200 and FLAG labeling. Interestingly, within the processes FLAG antibody revealed distinct clusters, suggesting that ND4 fusion proteins could be asymmetrically distributed along them. Additionally, Figure 2C illustrates that of the RGCs isolated from eyes electroporated with mutant *ND4*, those that were able to develop long neuritic processes did not express the human *ND4* gene. This result indicated a correlation between mitochondrial accumulation of the mutated ND4 protein in RGCs and their inability to grow neuritic processes in culture.

### Expression of Mutant ND4 Had a Deleterious Effect on RGCs In Vivo

To confirm in vivo expression of *ND4* genes, we examined cryostat retinal sections from animals sacrificed 25 days after in vivo ELP by immunochemistry with FLAG, NF200, GFP, and BRN3a antibodies. Cells in the GCL showed strong immunoreactivity to anti-FLAG in the cytoplasm, especially around the nuclei and along the axons (Figure 3A, ND4-FLAG). Figure 3A also illustrates a significant colocalization between FLAG and NF200 antibodies, as observed in cultured RGCs (Figure 2). Retinal sections immunolabeled with GFP and BRN3a antibodies consistently showed a diminution of BRN3a-postive cells in eyes electroinduced with mutant *ND4* (Figure 3B, *G11778A-ND4*). To evaluate this effect quantitatively, we counted BRN3a-positive cells in 24 animals in which one

the cytosol and along neuritic processes. The scale bar corresponds to 25 µm (magnification of 200×). A high-power view (magnification of 630×) featuring immunolabeled cells is also presented for each condition; scale bars represent 8 µm.
In both (A) and (B), arrows indicate either RGC somas lacking neuritic extensions or isolated neurites that were not associated with RGC nuclei. These signals have been often found in eyes electroporated with mutant *ND4*, indicating its deleterious effect on RGC survival ex vivo.
(C) A retinal ganglion cell purified from eyes electroporated with mutant *ND4*, which developed long neuritic processes, is shown. This RGC did not immunostain with anti-FLAG antibody, indicating that it did not express mutant *ND4*. The bar corresponds to 25 µm (magnification of 200×). In the bottom of the image, a RGC with two short neurites is also shown, this cell was immunolabeled with anti-FLAG antibody, indicating the expression of mutant *ND4*. Scale bars represent 25 µm. A high-power view (magnification of 630×) featuring the two RGCs immunolabeled with the antibodies is also presented; scale bars represent 8 µm.
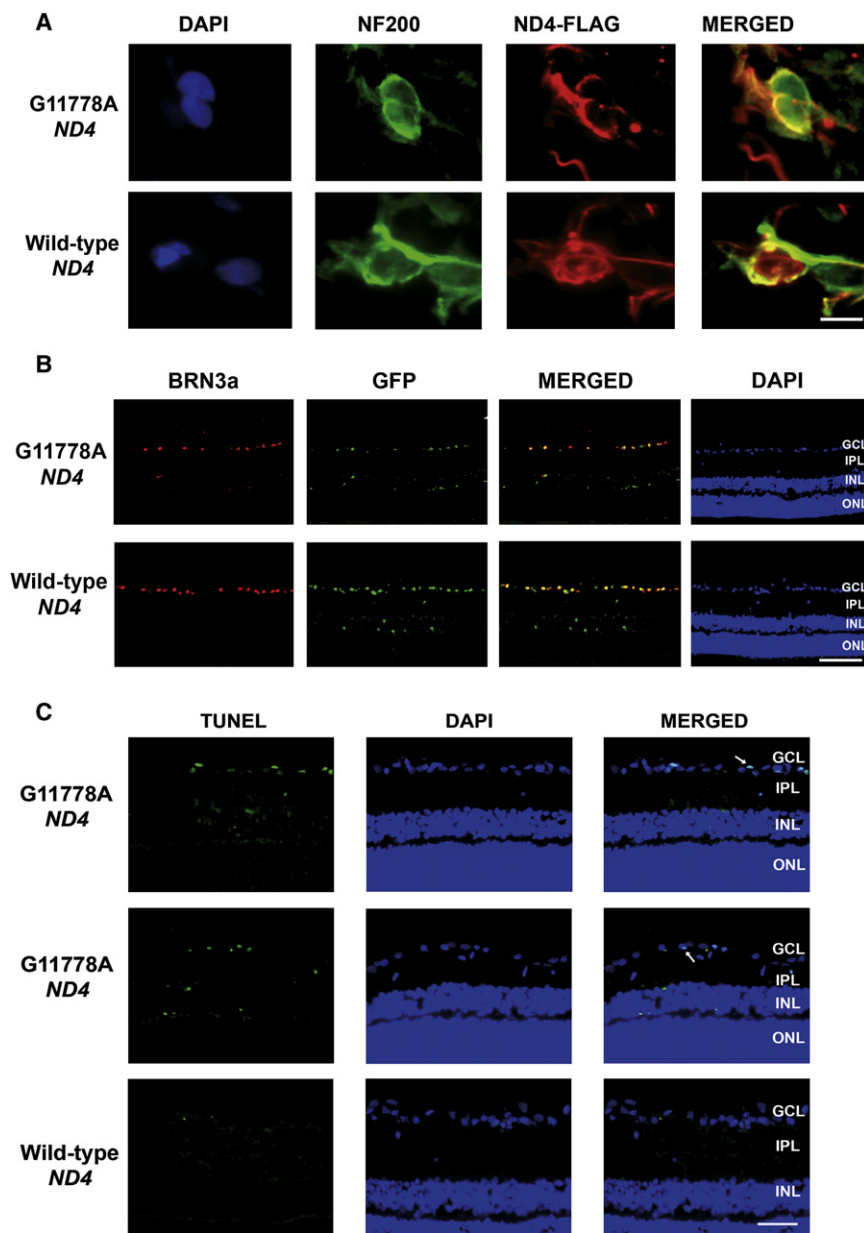
Figure 3. In Vivo Expression of Mutant ND4

(A) Immunofluorescence analyses with antibodies against the NF200 protein and the FLAG epitope were performed on cryostat retinal sections from animals electroporated with either mutant (G11778A ND4) or the wild-type ND4 gene and sacrificed 25 days later. The image illustrates cells strongly immunostained with NF200 in the GCL, indicating that they were RGCs. The signal was essentially visualized along cell axons and around the nuclear envelops but was excluded from the nucleus (DAPI). As we observed in cultured RGCs (Figure 2) ND4 fusion proteins presented the same subcellular distribution than NF200, illustrated by the significant colocalization of both Flag and NF200 signals (MERGED). A magnification of 630× is shown; the scale bar corresponds to 10 μm.

(B) The effect of in vivo ELP on RGC viability was assessed by immunostaining with BRN3a for labeling ganglion cell nuclei and with GFP for labeling electroinduced cells. The number of RGC-positive cells were estimated with merged images of BRN3a and DAPI stainings. It clearly appeared that the number of RGCs was strongly reduced when the eyes expressed mutant ND4 (G11778A ND4) in comparison to when eyes were electroporated with wild-type ND4. Retinal sections shown correspond to animals sacrificed 25 days after in vivo ELP. Scale bars represent 50 μm (magnification of 200×). GCL, ganglion cell layer; IPL, inner plexiform layer; INL, inner nuclear layer; and ONL, outer nuclear layer.

(C) Retinas were assessed for TUNEL labeling after in vivo ELP with either mutant (G11778A ND4) or wild-type ND4 vector. The frequency of TUNEL-positive cells was greater in the GCL of retinas expressing mutant ND4 (G11778A ND4) than in retinas expressing its wild-type counterpart (wild-type ND4). The intensity of staining and the number of cells displaying advanced apoptotic features (arrows) was increased in retinas expressing mutant ND4. Some cells showed preferential staining of chromatin in the proximity of the nuclear envelop, a feature of early-stage apoptosis (arrows). Rarely, few TUNEL-positive cells were evidenced in the INL of animals electroporated with mutant ND4, suggesting that amacrine cells expressing mutant ND4 could undergo apoptosis. Scale bars represent 25 μm (magnification of 400×). GCL, ganglion cell layer; IPL, inner plexiform layer; INL, inner nuclear layer; and ONL, outer nuclear layer.

eye was electroporated with mutant ND4 and compared this number to counts from (i) 11 animals electroporated in one eye with wild-type ND4 and (ii) 14 animals electroporated in one eye with the empty vector (GFP). Table 1 shows the mean number of BRN3a-positive cells for four independent retinal sections per animal in comparison to the total amount of DAPI-stained nuclei in the GCL. The number of BRN3a-positive cells in retinas expressing mutant ND4 was approximately 30% lower than in retinas expressing either wild-type ND4 or GFP. This result was

highly significant according to a Student's t test (p = 1.6 × 10^{-05} for *G11778A-ND4/WT-ND4* groups and p = 3.8 × 10^{-05} for *G11778A-ND4*/GFP groups). Moreover, the RGC number diminution was accompanied by a 13% decrease in DAPI-stained cells in the GCL (Table 1). This decrease was also significant: p = 0.04 for *G11778A-ND4/WT-ND4* groups and p = 0.05 for *G11778A-ND4*/GFP groups. Importantly, the wild-type ND4 gene transduction did not compromise RGC viability. Indeed, there was significant difference neither in the number of RGCs nor in

Table 1. Overall Number of RGCs in Retinal Sections of Electroporated Eyes after 25 Days of Transgene Expression

	GFP n = 14	G11778A-*ND4* n = 24	Wild-Type *ND4* n = 11
Overall number of RGCs	292 ± 21	197 ± 13	274 ± 14
Total number of cells in the GCL	1086 ± 52	966 ± 51	1118 ± 68

RGCs were counted after immunolabeling with BRN3a antibody. The RGC and total cell numbers presented in the table represent the means ± SEM obtained after all of the BRN3a and DAPI-positive cells in the GCL were counted in four independent retinal sections per animal.

the overall amount of cells in the GCL when the eyes were electroporated with GFP or wild-type-*ND4* vectors (Table 1, p = 0.36). Thus, the negative impact on RGC survival is the direct consequence of mutant *ND4* allotopic expression.

Next, we performed a TUNEL assay on retinal sections from six animals 25 days after in vivo ELP with either wild-type or mutant *ND4* vectors (Figure 3C). Eyes electroporated with the wild-type gene were almost TUNEL-negative; out of four independent retinal sections per animal the average number of positive cells was 1.5 ± 0.8. In contrast, the fraction of TUNEL-positive cells in the GCL was 12-fold higher (18 ± 5) in eyes that were electroporated with mutant *ND4*, and TUNEL labeling in the GCL was consistently observed (Figure 3C). This difference was significant according to a Student's t test (p = 0.0055; n = 6). Interestingly, the TUNEL-positive cells had a diverse range of morphology. Some cells displayed densely stained nuclei, whereas others showed preferential staining of chromatin close to the nuclear periphery; such staining could indicate an early stage of apoptosis (Figure 3C, arrows). The above results indicate that the expression of mutant *ND4* induced neuronal cell death in the GCL, consistent with the significant reduction of RGC counts in retinal sections (Table 1).

RGC Loss Induced by Mutant *ND4* Was Rescued by Introduction of the Wild-Type Gene

Because in vivo transgene expression was stable for up to 50 days, we attempted to prevent RGC loss in animals that had expressed mutant *ND4* for 14 days by performing a second ELP with its wild-type counterpart. Then, animals were examined 31 days later (day 45), when it was expected that a large number of RGCs would simultaneously express both versions of *ND4*. First, we measured RGC loss at 14 and 48 days after in vivo ELP. Retinas from five animals sacrificed 14 days after ELP with mutant *ND4* gene did not show significant differences in the number of RGCs (Table 2, p = 0.45). The number of RGCs was also determined in eight animals after 48 days of mutant *ND4* expression and in 23 animals that expressed wild-type *ND4* for 48 days. In those animals that expressed mutant *ND4* animals for 48 days, an approximate 38% decrease in RGC counts was observed in comparison to when

wild-type *ND4* was expressed. This difference was highly significant according to a Student's t test (p = 3.9×10^{-8}).

Next, eyes from 18 animals were subjected to a first ELP with mutant *ND4*. After 2 weeks, eyes expressing mutant *ND4* were subjected to a second ELP with the wild-type gene. Thirty-one days later, the animals were sacrificed, and RGCs were counted. The transduction of wild-type *ND4* in RGCs at day 14 significantly prevented RGC loss in vivo; total numbers of RGCs were not statistically different between eyes electroporated twice and rat eyes that received only wild-type *ND4* (Table 2, p = 0.19). Moreover, the highly significant difference between RGC numbers in these animals relative to animals that expressed mutant *ND4* for 48 days (Table 2; p = 2×10^{-6}) demonstrated the beneficial effect of wild-type *ND4* expression on RGC survival.

To confirm that the neuroprotection observed was the direct consequence of wild-type *ND4* gene expression, we subjected eight animals that expressed mutant *ND4* for 14 days to a second ELP with the GFP vector and performed RGC counts 31 days later. It was clear that GFP expression did not protect RGCs because their number was reduced by almost 40% (Table 2). The total number of cells in the GCL, estimated by DAPI labeling, in animals electroporated with the mutant *ND4* genes or mutant *ND4* + GFP appeared diminished in comparison to cells counted in eyes electroporated with wild-type *ND4*. However, the decrease was statistically significant only for eyes electroporated with both mutant *ND4* and GFP (Table 2, p = 0.02). There was no significant difference between the overall number of cells in the GCL of animals expressing mutant *ND4* and the number in animals expressing both mutant *ND4* and GFP (p = 0.27), arguing against the possibility that the second round of ELP with the GFP damaged the GCL. Furthermore, total cell number in the GCL was quite similar in eyes electroporated with wild-type *ND4* and eyes electroporated with both mutant and wild-type *ND4* (Table 2, p = 0.8), thus indicating that treatment at day 14 with wild-type *ND4* halted cell loss in the GCL.

For examination of a possible association between RGC soma loss estimated by immunostaining for BRN3a (Tables 1 and 2) and changes in RGC intraretinal axons, retinal whole mounts from controls or animals subjected to in vivo ELP were processed for immunohistochemistry with NF200 (Figure 4). It clearly appeared that very few axon profiles were visible in retinas in which in vivo ELP was performed with mutant *ND4* (Figure 4A); conversely, the number of axons stained with NF200 was higher and comparable in retinas from eyes electroporated with either wild-type *ND4* or GFP (Figure 4A). Whole-mount retinas from eyes in which a second ELP was performed with either wild-type *ND4* or GFP were immunostained with NF200. Remarkably, the number of axons stained by NF200 was consistently higher when ELP was performed with wild-type *ND4* than when eyes were electroporated with GFP. Indeed, no noticeable difference in the staining was detected between whole-mount retinas from control

Table 2. Overall Number of RGCs in Retinal Sections of Electroporated Eyes

	Animals Sacrificed 14 Days after ELP		Animals Sacrificed 48 Days after a Unique ELP		Animals Sacrificed 45 Days after the First ELP	
	G11778A-*ND4* n = 5	Wild-type *ND4* n = 5	G11778A-*ND4* n = 8	Wild-type *ND4* n = 23	G11778A-*ND4* + Wild-type *ND4* n = 18	G11778A-ND4 + GFP vector n = 8
RGC number	292 ± 12	305 ± 12	183 ± 10	297 ± 10	276 ± 10	178 ± 10
Total cell number	1000 ± 35	1058 ± 46	977 ± 49	1033 ± 31	1020 ± 41	895 ± 42

RGCs were counted after immunolabeling with BRN3a antibody. DAPI staining allowed estimation of total nuclei in the GCL. Five animals were sacrificed 14 days after the electroinduction. Eight retinas were evaluated after long-term expression of mutant *ND4*, and 23 retinas were evaluated after long-term expression of its wild-type counterpart (48 days). Eighteen animals were subjected to two ELPs and sacrificed 31 days after the second intervention. First, they expressed for 14 days mutant *ND4*, and the same eye received its wild-type counterpart. Eight additional rats were subjected to two ELPs, the first one with mutant *ND4* and 14 days later with the GFP vector. The RGC and total cell numbers presented in the table represent the means ± SEM obtained after all of the BRN3a and DAPI-positive cells in the GCL were counted for four independent retinal sections per animal.

eyes and those from eyes electroporated first with mutant *ND4* and then with its wild-type counterpart (Figure 4B). These data indicated that RGC axon degeneration was prevented in animals subjected to a second ELP with wild-type *ND4*.

## Functional Assessment of Visual Responses in Animals Expressing Mutant *ND4*

The functional impact of RGC loss due to the expression of mutant *ND4* was assessed by optomotor head-tracking experiments in 12-week-old pigmented Long Evans rats.[21,23] Tracking capability was examined in both clockwise and counterclockwise drum rotations at three spatial frequencies. Because only temporal-to-nasal motion is effective through each eye, clockwise movement will drive tracking through the left eye, whereas counterclockwise motion will activate the right eye.[23] Therefore, we were able to independently assess vision of the two animal eyes.

Ten control rats, eight animals that had expressed for 25 days in their right eyes wild-type *ND4*, and ten animals that had expressed mutant *ND4* in the same eye for the same period were subjected to the test. Figure 5A shows no significant difference between clockwise and counterclockwise responses in control animals for any of the spatial frequencies monitored (Student's t test; p = 0.97, 0.23, and 0.42 for 0.125, 0.25, and 0.5 cyc/deg, respectively). Animals expressing the wild-type *ND4* gene mostly presented head-tracking scores of a magnitude similar to that of control animals (Figure 5B), and as in controls, scores were not significantly different for the clockwise and counterclockwise drum rotations (Student's t test; p = 0.6, 0.92, and 0.22 for 0.125, 0.25, and 0.5 cyc/deg, respectively). Animals expressing mutant *ND4* performed significantly worse at all frequencies for the counterclockwise drum rotation but performed similarly to controls and animals expressing wild-type *ND4* in the clockwise drum rotation (Figure 5C). The decline in visual performance of these animals, scored for the counterclockwise drum rotation, was statistically different for each spatial frequency of visual stimuli (Student's t test; p = 0.0075, 0.011, and 0.0065 for 0.125, 0.25, and 0.5 cyc/deg, respectively). As expected, the optomotor responses for the counterclockwise rotation were significantly different in eyes electroporated with

mutant *ND4* than in untreated eyes or in eyes electroporated with wild-type *ND4*. For instance, at the spatial frequency of 0.125 cyc/deg, comparisons of the *G11778A-ND4*/control group and the *G11778A-ND4*/*WT-ND4* group gave p values of 0.015 and 0.018, respectively. To evaluate whether the neuroprotection achieved by the second ELP with wild-type *ND4* (Table 2 and Figure 4) led to visual function benefits, we monitored head-tracking performance in ten rats subjected to a second ELP with wild-type *ND4* 14 days after the first intervention in their right eyes with mutant *ND4*. The second ELP prevented the loss of visual function, and indeed, counterclockwise scores for the three frequencies examined were higher than those measured in animals in which only mutant *ND4* was expressed (Figure 5D). For instance, the acuity score measured in these rats was 77% of that measured for the accompanying untreated eyes for the spatial frequency of 0.125 cyc/deg for the counterclockwise drum rotation. This was significantly better (p = 0.00032) than tracking scores for animals electroporated with mutant *ND4* (Figure 5C; 17.8% of that measured in the accompanying untreated eyes).

To further confirm the deleterious effect of mutant *ND4* expression on visual function, we performed optomotor head-tracking experiments in four animals that expressed mutant *ND4* in their left instead of right eyes (Table 3). Animals did not exhibit much tracking at any frequency with clockwise stimulus motion, implying poor visual acuity in their left eyes. Conversely, when the motion was reversed, tracking was normal, and scores recorded for these animals were similar to those for control rats or animals electroporated with wild-type *ND4* (Figure 5A and 5B). Thus, a direct link exists between mutant *ND4* expression and decreased visual capabilities independently of which eye was treated. Moreover, four animals subjected to two ELPs in their left eyes showed a clear improvement in their visual responses for clockwise drum rotation; indeed, in contrast to animals subjected to a unique ELP, these animals tracked significantly better in all frequencies monitored for the clockwise stimulus motion (Table 3).

Therefore, expression of wild-type *ND4* unambiguously preserved visual function in animals that expressed mutant *ND4* for 14 days, and this was certainly correlated to
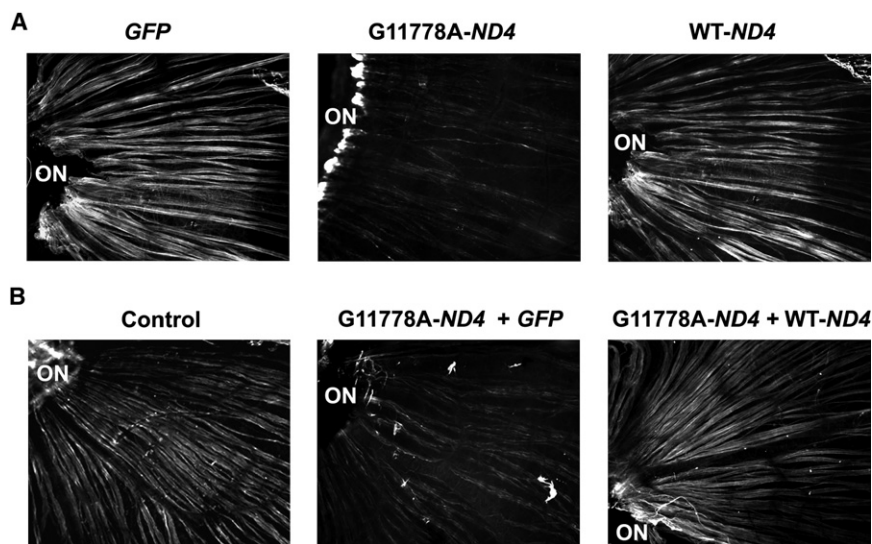
Figure 4. NF200-Labeled Axons in Whole-Mmount Retinas

(A) Immunostaining with NF200 in whole-mount retinas from animals subjected to a unique ELP clearly showed many fewer NF200-positive axons when animals were electroinduced with mutant *ND4* (G11778A-*ND4*) than when both retinas expressed either the empty vector (GFP) or the wild-type gene (WT-*ND4*).

(B) Retinal flat-mount labeled with NF200 from a control animal (13 weeks old) was compared to the labeling obtained in animals electroporated twice. It clearly appeared that when the second ELP was performed with wild-type *ND4* there was good axon preservation (G11778A-*ND4* + WT-*ND4*), whereas relatively poor preservation was seen in the GFP-treated retina (G11778A-*ND4* + GFP), similar to the one observed when a unique ELP was performed with mutant *ND4* (A). A magnification of 200× is shown. ON, optic nerve.

the prevention of RGC soma and intraretinal-axon loss demonstrated in vivo after the second ELP (Table 2 and Figure 4).

Discussion

Because of the multiplicity of mitochondrial functions, ranging from intermediate metabolism to energy production and apoptosis, there exist many potential avenues whereby damaged mitochondria can compromise cell survival. Extensive research efforts aimed at deciphering the molecular basis of mitochondria implication in human diseases are currently underway worldwide. However, the impact of these efforts on the identification of valuable remedies is very limited, and we are still unable to treat mitochondrial diseases.[5] A recent review has evaluated randomized and quasi-randomized trials comparing pharmacological (vitamins) and nonpharmacological (food supplements) approaches as well as physical training in patients with mitochondrial disorders. The authors concluded that there is currently no clear evidence supporting the use of any intervention in mitochondrial disorders and that further research is needed to establish the role of a wide range of therapeutic approaches.[28] Within this context, mtDNA-related disorders encompass an increasing number of clinical pictures due to more than 300 different provisional or confirmed pathogenic changes in mtDNA.[29] Gene therapy for mtDNA-related diseases presents four major problems: (1) the nature of an efficient protocol that takes into account the unique properties of mtDNA (heteroplasmy, polyplasmy) and the hydrophobic nature of the 13 proteins encoded by the organelle genome; (2) the lack of suitable animal models for testing and validating new therapies; (3) the inability to manipulate the mito-

chondrial genome inside the organelle of living cells; (4) as for any Mendelian disorder, the choice of vectors, delivery method, and dose/toxicity studies.

Vision impairment is a prevalent feature in mitochondrial diseases; indeed, retina cells contain a large number of mitochondria, reflecting their high energy requirements.[30] Moreover, mitochondrial dysfunction may contribute to changes in macular function observed in aging and age-related macular degeneration.[31] Because the eye has a delimited and highly isolated structure, immunoprivilege, and accessibility, it is a particularly promising organ with respect to gene therapy.[32] Hence, two groups recently described the first results of clinical trials investigating the short-term safety and preliminary efficacy of gene therapy for Leber's congenital amaurosis type II (LCA, [MIM 204100]), a severe early-onset retinal degeneration due to mutations in the *RPE65* gene (MIM +180069).[33] The patients were enrolled in trials of recombinant adeno-associated virus (rAAV) delivery of the human *RPE65* [MIM + 180069]. The data suggested that in the short-term, the procedure is safe and efficient and provided the foundation for gene therapy approaches to the treatment of LCA and possibly other forms of retinal degeneration.[34,35]

Our main objective is to develop a gene therapy that could be both preventive and curative for optic neuropathies due to mitochondrial dysfunction. In this pursuit, we focused on the LHON disease due to known mutations in mtDNA. Disease onset in the majority of cases is between 15 and 35 years of age, but with the availability of the molecular diagnosis, early or late cases are increasingly reported.[10,36] LHON typically manifests as acute or subacute bilateral loss of vision. Visual loss often occurs asynchronously over the course of several weeks to months.[10,37] Some patients continue in a "chronic" state characterized by a low-grade degenerative process that may consistently
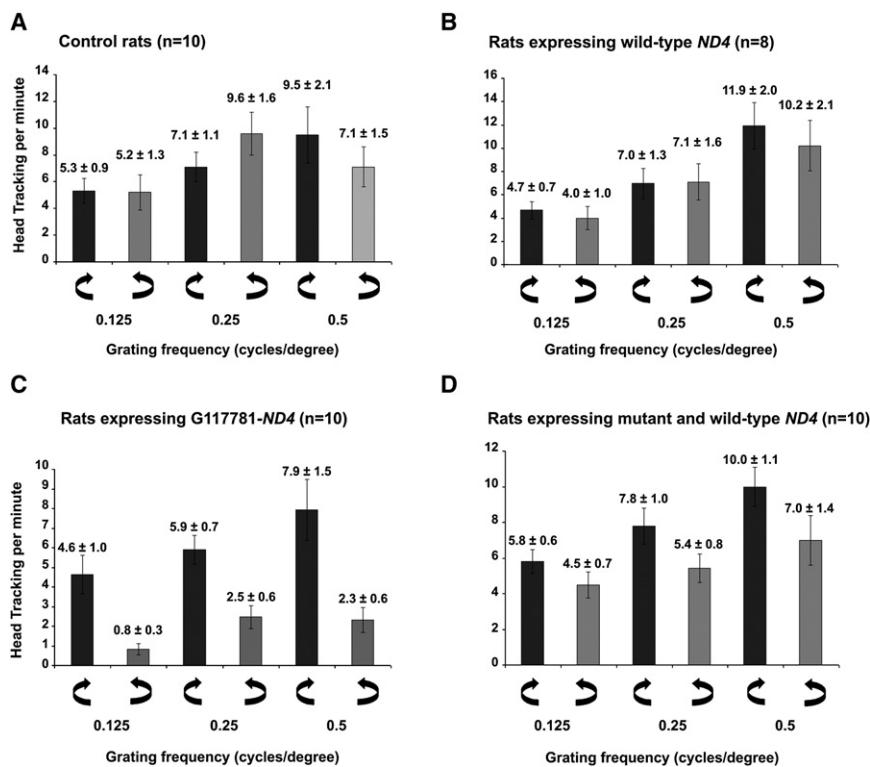
Figure 5. Assessment of Visual Function via Optomotor Tests of Long Evans Rats

(A) Head-tracking responses of ten controls (8 and 12 weeks old) compared with rats electroporated in their right eyes with the wild-type *ND4* gene (B). The three grating frequencies of 0.125, 0.25, and 0.5 cyc/deg are shown in both clockwise (arrows revolving in clockwise direction) and counterclockwise (arrows revolving in counterclockwise direction) directions of motion. Visual thresholds in these animals did not depend on the direction of rotation given that no significant difference was measured in the three grating frequencies monitored. Moreover, the scores were comparable in all the rats assessed, indicating that electroporation with wild-type *ND4* (B) did not compromise visual acuity.

(C) Optomotor tracking in ten animals subjected to in vivo ELP with mutant *ND4*. In vivo ELP in the right eye with mutant *ND4* strongly diminished tracking when the grating motion was counterclockwise but had no effect on clockwise tracking. According to a Student's t test, a significant difference was measured in the three grating frequencies monitored, indicating a link between mutant *ND4* expression and the loss of visual function.

(D) Ten animals were subjected to a second ELP with wild-type *ND4* 14 days after mutant *ND4* expression in their right eyes. Head-tracking responses in the counterclockwise motion were significantly better in these animals than in those subjected to a single ELP with mutant *ND4*. For instance, comparative analyses of means tracking in the 0.125 cyc/deg grating frequency of clockwise and counterclockwise responses were not statically different according to a Student's t test (p = 0.1).

For animals subjected to ELP, all the assessments were performed 25 and 35 days after the intervention, and values presented are the means ± SEM of these two assessments.

worsen the residual vision over the years.[37] Hence, the acutely symptomatic LHON patient with monocular vision loss provides a unique clinical situation in which it becomes possible not only to test a therapeutic agent during the critical window before vision is lost in the second eye but also to prevent the progressive worsening of visual function.

We have developed an approach of gene therapy that successfully restores OXPHOS dysfunction in preclinical models for three different mtDNA gene mutations. Our optimized allotopic expression vectors allowed the replacement of defective proteins in fibroblasts harboring 100% of mutated mtDNA molecules in *ATP6*, *ND4*, or *ND1* genes.[15,16] Thus, we have created in these cells a situation often found in patient tissues, where mutated and wild-type mtDNAs coexist in various proportions (heteroplasmy). It has been clearly demonstrated that the percentage of mutated forms contributes to disease expression in patients and that symptoms only appear above threshold levels of mutant mtDNA molecules.[1,3] With our approach, we have forced the system into reverse by expressing wild-type mitochondrial genes to push the proportion of the mutant form below the threshold for pathology. The key to our approach has been the inclusion in the expression vectors of the *COX10*-3′ UTR, which allows the sorting to the mitochondrial surface of mRNAs and maximizes unequivocally mitochondrial translocation of these highly hydrophobic proteins.[15,16] Henceforth, this innovation makes feasible the prospect of gene therapy for mtDNA-related diseases and circumvents the limitations encountered to date.[13,14] Recently, Qi and colleagues showed that the allotopic expression of a nuclear version of the mutant *ND4* gene in mouse eyes led to RGC and optic-nerve degeneration, and these mice can be used for testing the effectiveness of treatments for LHON.[38] Nevertheless, their approach could encounter the limitation of the inefficient mitochondrial import of the hydrophobic ND4 protein because the corresponding mRNA was not sorted to the mitochondrial surface. Transgene expression could thus become potentially toxic for mouse retina over time, preventing the generation of a robust mouse model of LHON. In our study, the highest effectiveness for mitochondrial dysfunction rescue was achieved when both the MTS and 3′ UTR of *COX10* were combined with wild-type genes.[15] These findings confirmed our previous data in HeLa cells: The amount of fully mitochondrially translocated ATP6 protein was around 2-fold higher when the nuclearly recoded *ATP6* gene was associated with both

Table 3. Optomotor Tests of Animals Electroporated in Their Left Eyes

Gratings frequency (cycles per degree)	Animals Electroporated Once in Their Left Eyes with G11778A-*ND4* n = 4			Animals Electroporated Twice in Their Left Eyes with G11778A-*ND4* + Wild-Type *ND4* n = 4		
	0.125	0.25	0.5	0.125	0.25	0.5
Clockwise	0.83 ± 0.26	1.88 ± 0.46	2.5 ± 1.1	3 ± 0.7	4.5 ± 1.3	7.4 ± 0.8
Counterclockwise	5.5 ± 0.6	6.3 ± 0.85	8.2 ± 0.45	3.7 ± 1	5 ± 1.1	9.6 ± 0.7

Four animals were subjected to ELP with mutant *ND4* in their left eyes. A significant distinction between clockwise and counterclockwise tracking performances was observed: $p = 0.003$, 0.009, and 0.01 for gratings 0.125, 0.25, and 0.5 cyc/deg, respectively. Thus, performances were poor at any frequency for clockwise stimulus motion. An additional group of four rats was subjected to ELP with mutant *ND4*, and 14 days later a second ELP was performed with wild-type *ND4*. For frequencies of 0.125 and 0.25 cyc/deg , there were no significant differences between clockwise and counterclockwise tracking signals ($p = 0.72$ and 0.33, respectively) in animals subjected to two ELPs. At 0.5 cycles per degree, $p = 0.04$, but clockwise scores were 77% of the value measured in the counterclockwise rotation, as opposed to 30.5% in rats expressing mutant *ND4* only. Values represented in the table are the means ± SEM obtained for the eight animals subjected to optomotor tests twice.

the MTS and 3′ UTR of *SOD2* [MIM *147460] than when just the MTS was present in the construct.[39] Moreover, Bokori-Brown and Holt attempted to correct mitochondrial dysfunction in cells expressing the T8993G in *ATP6* by using a nuclearly encoded human *ATP6* gene linked to the MTS of bovine flavoprotein subunit of complex II, SDH_L. They were unsuccessful in that transgene expression was deleterious overtime and none of the transformed cells retained the vector two months after transfection. One hypothesis that could explain these data is that mRNA sorting to the mitochondrial surface is essential for ensuring the import of its protein inside the organelle. Thus, if mRNA is translated somewhere else in the cytosol, high levels of misfolded hydrophobic protein could accumulate and lead to progressive decline in cell fitness.

In the present study, we were able to create an animal model resembling LHON disease by taking advantage of the specific features of mtDNA genetics regarding heteroplasmy and by using our optimized allotopic-expression approach. Rat retinal ganglion cells (RGCs) that expressed in vivo the human *ND4* gene harboring the deleterious G11778A mutation carried a heteroplasmy due to the coexistence of the endogenous wild-type gene and the mutant *ND4* gene of our vector. Rat and human ND4 proteins differ by only 39 amino acids out of 459, and their identity and strong similarity degrees are of 68% and 20%, respectively, indicating that human ND4 proteins could integrate rat respiratory chain complex I. We performed in vivo electroporation in animal eyes to introduce *ND4* transgenes in RGCs.[17] More than 70% of RGCs expressed them for up to 50 days. Semiquantitative RT-PCR analyses performed in RGC cells purified from eyes electroporated with either wild-type or mutant *ND4* showed that corresponding mRNAs were as abundant as β-actin and *IGF1* mRNAs, two nuclearly transcribed molecules. Transgene mRNA steady-state levels could have been underestimated because RNAs were purified from the total RGC population, in which not all expressed the transgenes. However, we evaluated the impact of the coexistence of wild-type and mutant *ND4* genes for RGC function and viability in the experimental model generated. These animals reproduced morphological and functional features of the LHON pathology. Both the degeneration of RGC somas and the severe reduction of RGC intraretinal axons reflected selective death of ganglion cells and therefore recapitulated one of the pathology hallmarks. Ultimately, compromised RGC function would lead to optic-nerve atrophy and central vision loss as described in patients suffering from LHON. Remarkably, we were able to measure a significant decline of visual performance in animals expressing mutant *ND4*; this decline resembled devastating and sudden visual loss in young adulthood. Moreover, the deleterious impact of the allotopically expressed mutant *ND4* on RGCs was clearly demonstrated ex vivo; both RGC survival and ability to outgrowth neuritic processes were compromised. The deleterious consequences of mutant *ND4* expression for RGC survival were examined in a large number of animals: 24 and eight animals that expressed the transgene for 25 and 48 days, respectively. RGC counts undertaken in these animals revealed a significant 30% and 38% decrease, respectively, when these animals were compared to 12 age-matched controls, 34 animals electroporated with wild-type *ND4*, or 14 animals electroporated with the GFP vector. Hence, RGC injury due to mutant *ND4* expression was more severe when animals were sacrificed 48 days after in vivo ELP than when they were sacrificed at day 25. These data indicated that human ND4 protein was imported into mitochondria of RGCs and perturbed its function, either by a direct competition with the endogenous protein or by an impairment of respiratory chain complex activity and/or assembly. Unfortunately, it will be extremely difficult to determine which mechanism is responsible of our findings at the molecular level. Indeed, a very large number of rat RGCs are required for respiratory chain complex activity measurements or Blue Native Electrophoresis,[14] which would provide compelling evidence of effective mitochondrial import and assembly of allotopically expressed gene product in respiratory chain complex I. Nevertheless, the strong correlation between mutant *ND4* expression and impaired visual function encouraged us to pursue the exploration of this experimental model.

Because in vivo ELP led to stable transgene expression for up to 50 days and, most importantly, because mutant *ND4* expression was harmless during the first 14 days, we performed a second intervention in animal eyes by using the wild-type *ND4* gene in an attempt to prevent RGC degeneration and the loss of visual function. In 18 animals examined, wild-type *ND4* expression significantly protected RGCs, as measured by BRN3a immunostaining and by the estimation of intraretinal axons in whole-mounted retinas. These findings were correlated with the preservation of visual function in ten of these animals without unwanted harm or effects on animals or their eyes. The high efficiency of neuroprotection achieved by the second round of ELP might seem surprising; indeed, no significant differences were found between RGC counts in 18 animals subjected to two ELPs and 23 animals electroporated with wild-type *ND4* (Table 2, 7% fewer RGCs in animals subjected to two ELPs). However, the neuroprotection, as determined by the visual acuity in the injected eyes compared to the accompanying untreated eyes of these animals, was of 72% or 83% when right or left eyes were subjected to two rounds of ELP. Therefore, visual function was highly preserved, although it did not remain at 100%. One hypothesis that could explain the impressive prevention of RGC and visual-function loss achieved by the second ELP with wild-type *ND4* is that cells that were electropermeabilized during the first intervention could be more susceptible to the second one. Hence, we could obtain more than an additive effect for wild-type *ND4* treatment, and a very high proportion of cells expressing mutant *ND4* were successfully electropermeabilized and received large amounts of wild-type *ND4*. Multiple ELPs (up to six within an interval of a few weeks) have often been applied safely in vivo for both cancerologic and immunologic purposes and led to much more efficient results than a single treatment.[40,41]

In conclusion, we have created a valid animal model of LHON, and we were able both to prevent animals from becoming blind and to avoid toxicity. These data represent a breakthrough for the generation of a treatment aimed at improving life conditions of patients suffering from optic neuropathies with a mitochondrial etiology. The next step toward our goal of clinical trials for preventing blindness in patients suffering from LHON disease will be to assess the long-term safety of the optimized allotopic-expression approach with respect to retinal morphology and function in large animals by using rAAV-mediated gene therapy, as recently described.[42]

Supplemental Data

Supplemental Data include one table and are available online at http://www.ajhg.org/.

Acknowledgments

Web Resources

The URLs for data presented herein are as follows:

Online Mendelian Inheritance in Man (OMIM), http://www.ncbi.nlm.nih.gov/Omim/

MITOMAP: A Human Mitochondrial Genome Database. http://www.mitomap.org, 2008.

References

1. McFarland, R., Taylor, R.W., and Turnbull, D.M. (2007). Mitochondrial disease-its impact, etiology, and pathology. Curr. Top. Dev. Biol. *77*, 113–155.
2. Singh, K.K. (2006). Mitochondria damage checkpoint, aging, and cancer. Ann. N Y Acad. Sci. *1067*, 182–190.
3. Schapira, A.H. (2006). Mitochondrial disease. Lancet *368*, 70–82.
4. Schaefer, A.M., McFarland, R., Blakely, E.L., He, L., Whittaker, R.G., Taylor, R.W., Chinnery, P.F., and Turnbull, D.M. (2008). Prevalence of mitochondrial DNA disease in adults. Ann. Neurol. *63*, 35–39.
5. DiMauro, S., and Mancuso, M. (2007). Mitochondrial diseases: Therapeutic approaches. Biosci. Rep. *27*, 125–137.
6. Wallace, D.C., Singh, G., Lott, M.T., Hodge, J.A., Schurr, T.G., Lezza, A.M., Elsas, L.J. 2nd, and Nikoskelainen, E.K. (1988). Mitochondrial DNA mutation associated with Leber's hereditary optic neuropathy. Science *242*, 1427–1430.
7. Man, P.Y., Griffiths, P.G., Brown, D.T., Howell, N., Turnbull, D.M., and Chinnery, P.F. (2003). The epidemiology of Leber hereditary optic neuropathy in the North East of England. Am. J. Hum. Genet. *72*, 333–339.
8. Huizing, M., Brooks, B.P., and Anikster, Y. (2005). Optic atrophies in metabolic disorders. Mol. Genet. Metab. *86*, 51–60.
9. Abu-Amero, K.K., and Bosley, T.M. (2006). Mitochondrial abnormalities in patients with LHON-like optic neuropathies. Invest. Ophthalmol. Vis. Sci. *47*, 4211–4220.
10. Yen, M.-Y., Wang, A.-G., and Wei, Y.-H. (2006). Leber's hereditary optic neuropathy: A multifactorial disease. Prog. Retin. Eye Res. *25*, 381–396.
11. Manfredi, G., Fu, J., Ojaimi, J., Sadlock, J.E., Kwong, J.Q., Guy, J., and Schon, E.A. (2002). Rescue of a deficiency in ATP synthesis by transfer of MTATP6, a mitochondrial DNA-encoded gene to the nucleus. Nat. Genet. *30*, 394–399.
12. Guy, J., Qi, X., Pallotti, F., Schon, E.A., Manfredi, G., Carelli, V., Martinuzzi, A., Hauswirth, W.W., and Lewin, A.S. (2002). Rescue of a mitochondrial deficiency causing Leber Hereditary Optic Neuropathy. Ann. Neurol. *52*, 534–542.
13. Oca-Cossio, J., Kenyon, L., Hao, H., and Moraes, C.T. (2003). Limitations of allotopic expression of mitochondrial genes in mammalian cells. Genetics *165*, 707–720.

14. Bokori-Brown, M., and Holt, I.J. (2006). Expression of Alga1 nuclear ATP synthase subunit 6 in human cells results in protein targeting to mitochondria but no assembly into ATP synthase. Rejuvenation Res. *9*, 455–469.

15. Bonnet, C., Kaltimbacher, V., Ellouze, S., Augustin, S., Bénit, P., Forster, V., Rustin, P., Sahel, J.A., and Corral-Debrinski, M. (2007). Allotopic mRNA localization to the mitochondrial surface rescues respiratory chain defects in fibroblasts harboring mtDNA mutations affecting complex I or V subunits. Rejuvenation Res. *10*, 127–144.

16. Bonnet, C., Augustin, S., Ellouze, S., Bénit, P., Bouaita, A., Rsutin, P., Sahel, J.-A., and Corral-Debrinski, M. (2008). The optimized allotopic expression of ND1 or ND4 genes restores respiratory chain complex I activity in fibroblasts harboring mutations in these genes. Biochim. Biophys. Acta.. In press. Published online May 6, 2008. 10.1016/j.bbamcr.2008.04.018.

17. Ishikawa, H., Takano, M., Matsumoto, N., Sawada, H., Ide, C., Mimura, O., and Dezawa, M. (2005). Effect of GDNF gene transfer into axotomized retinal ganglion cells using in vivo electroporation with a contact lens-type electrode. Gene Ther. *12*, 289–298.

18. Danias, J., Shen, F., Goldblum, D., Chen, B., Ramos-Esteban, J., Podos, S.M., and Mittag, T. (2002). Cytoarchitecture of the retinal ganglion cells in the rat. Invest. Ophthalmol. Vis. Sci. *43*, 587–594.

19. Barres, B.A., Silverstein, B.E., Corey, D.P., and Chun, L.L. (1988). Immunological, morphological, and electrophysiological variation among retinal ganglion cells purified by panning. Neuron *1*, 791–803.

20. Fuchs, C., Forster, V., Balse, E., Sahel, J.A., Picaud, S., and Tessier, L.H. (2005). Retinal-cell-conditioned medium prevents TNF-alpha-induced apoptosis of purified ganglion cells. Invest. Ophthalmol. Vis. Sci. *46*, 2983–2991.

21. Cowey, A., and Franzini, C. (1979). The retinal origin of uncrossed optic nerve fibres in rats and their role in visual discrimination. Exp. Brain Res. *35*, 443–455.

22. Coffey, P.J., Girman, S., Wang, S.M., Hetherington, L., Keegan, D.J., Adamson, P., Greenwood, J., and Lund, R.D. (2002). Long-term preservation of cortically dependent visual function in RCS rats by transplantation. Nat. Neurosci. *5*, 53–56.

23. Douglas, R.M., Alam, N.M., Silver, B.D., McGill, T.J., Tschetter, W.W., and Prusky, G.T. (2005). Independent visual threshold measurements in the two eyes of freely moving rats and mice using a virtual-reality optokinetic system. Vis. Neurosci. *22*, 677–684.

24. Xiang, M., Zhou, L., Macke, J.P., Yoshioka, T., Hendry, S.H., Eddy, R.L., Shows, T.B., and Nathans, J. (1995). The Brn-3 family of POU-domain factors: primary structure, binding specificity, and expression in subsets of retinal ganglion cells and somatosensory neurons. J. Neurosci. *15*, 4762–4785.

25. Carelli, V., Ross-Cisneros, F.N., and Sadum, A.A. (2004). Mitochondrial dysfunction as a cause of neuropathies. Prog. Retin. Eye Res. *23*, 53–89.

26. Lin, B., Wang, S.W., and Masland, R.H. (2004). Retinal ganglion cell type, size, and spacing can be specified independent of homotypic dendritic contacts. Neuron *43*, 475–485.

27. Ruiz-Ederra, J., Garcia, M., Hicks, D., and Vecino, E. (2004). Comparative study of the three neurofilament subunits within pig and human retinal ganglion cells. Mol. Vis. *10*, 83–92.

28. Chinnery, P., Majamaa, K., Turnbull, D., and Thorburn, D. (2006). Treatment for mitochondrial diseases. Cochrane Database Syst. Rev. *1*, CD004426.

29. Ruiz-Pesini, E., Lott, M.T., Procaccio, V., Poole, J.C., Brandon, M.C., Mishmar, D., Yi, C., Kreuziger, J., Baldi, P., and Wallace, D.C. (2007). An enhanced MITOMAP with a global mtDNA mutational phylogeny. Nucleic Acids Res. *35*, D823–D828.

30. Perkins, G.A., Ellisman, M., and Fox, D.A. (2004). The structure-function correlates of mammalian rod and cone photoreceptor mitochondria: observations and unanswered questions. Mitochondrion *4*, 695–703.

31. Feher, J., Kovacs, I., Artico, M., Cavallotti, C., Papale, A., and Balacco Gabrieli, C. (2006). Mitochondrial alterations of retinal pigment epithelium in age-related macular degeneration. Neurobiol. Aging *27*, 983–993.

32. Bainbridge, J.W., Tan, M., and Ali, R.R. (2006). Gene therapy progress and prospects: The eye. Gene Ther. *13*, 1191–1197.

33. Hanein, S., Perrault, J., Gerber, S., Tanguy, G., Rozet, J.M., and Kaplan, J. (2006). Leber congenital amaurosis: survey of the genetic heterogeneity, refinement of the clinical definition and phenotype-genotype correlations as a strategy for molecular diagnosis. Clinical and molecular survey in LCA. Adv. Exp. Med. Biol. *572*, 15–20.

34. Maguire, A.M., Simonelli, F., Pierce, E.A., Pugh, E.N. Jr., Mingozzi, F., Bennicelli, J., Banfi, S., Marshall, K.A., Testa, F., Surace, E.M., et al. (2008). Safety and efficacy of gene transfer for Leber's Congenital Amaurosis. N. Engl. J. Med. *358*, 2240–2248.

35. Bainbridge, J.W., Smith, A.J., Barker, S.S., Robbie, S., Henderson, R., Balaggan, K., Viswanathan, A., Holder, G.E., Stockman, A., Tyler, N., et al. (2008). Effect of gene therapy on visual function in Leber's Congenital Amaurosis. N. Engl. J. Med. *358*, 2231–2239.

36. Carelli, V., La Morgia, C., Iommarini, L., Carroccia, R., Mattiazzi, M., Sangiorgi, S., Farne', S., Maresca, A., Foscarini, B., Lanzi, L., et al. (2007). Mitochondrial optic neuropathies: how two genomes may kill the same cell type? Biosci. Rep. *27*, 173–184.

37. Sadun, A.A., Salomao, S.R., Berezovsky, A., Sadun, F., Denegri, A.M., Quiros, P.A., Chicani, F., Ventura, D., Barboni, P., Sherman, J., et al. (2006). Subclinical carriers and conversions in Leber hereditary optic neuropathy: a prospective psychophysical study. Trans. Am. Ophthalmol. Soc. *104*, 51–61.

38. Qi, X., Lewin, A.S., Hauswirth, W.W., and Guy, J. (2007). The mutant human ND4 subunit of complex I induces optic neuropathy in the mouse. Invest. Ophthalmol. Vis. Sci. *48*, 1–10.

39. Kaltimbacher, V., Bonnet, C., Lecoeuvre, G., Forster, V., Sahel, J.A., and Corral-Debrinski, M. (2006). mRNA localization to the mitochondrial surface allows the efficient translocation inside the organelle of a nuclear recoded ATP6 protein. RNA *12*, 1408–1417.

40. Kaneda, T., Honda, A., Hakozaki, A., Fuse, T., Muto, A., and Yoshida, T. (2007). An improved Graves' disease model established by using in vivo electroporation exhibited long-term immunity to hyperthyroidism in BALB/c mice. Endocrinology *148*, 2335–2344.

41. Goto, T., Nishi, T., Kobayashi, O., Tamura, T., Dev, S.B., Takeshima, H., Kochi, M., Kuratsu, J.-I., Sakata, T., and Ushio, Y. (2004). Combination electro-gene therapy using herpes virus yhymidine kinase and interleukin-12 expression plasmids is highly efficient against murine carcinoma *in vivo*. Mol. Ther. *10*, 929–937.

42. Jacobson, S.G., Boye, S., Aleman, T.S., Conlon, T.J., Zeiss, C.J., Roman, A.J., Cideciyan, A.V., Schwartz, S.B., Komaromy, A.M., Doobrajh, M., et al. (2006). Safety in nonhuman primates of ocular AAV2–RPE65, a candidate treatment for blindness in Leber congenital amaurosis. Hum. Gene Ther. *17*, 845–858.